

Weak Localization and Weak Antilocalization in Double-Gate a-InGaZnO Thin-Film Transistors

Wei-Hsiang Wang, Elica Heredia, Syue-Ru Lyu, Shu-Hao Liu, and Pei-hsun Jiang*
Department of Physics, National Taiwan Normal University, Taipei 116, Taiwan

Po-Yung Liao and Ting-Chang Chang
Department of Physics, National Sun Yat-Sen University, Kaohsiung 804, Taiwan

We demonstrate manipulation of quantum interference by controlling the competitions between weak localization (WL) and weak antilocalization (WAL) via variation of the gate voltages of double-gate amorphous InGaZnO thin-film transistors. Our study unveils the full profile of an intriguing universal dependence of the respective WL and WAL contributions on the channel conductivity. This universality is discovered to be robust against interface disorder.

Measurements of magnetoconductivity are known to be a powerful tool to study spin effects. *Weak localization* (WL) refers to constructive quantum interference of coherently back-scattered conduction electrons, which leads to a suppressed conductivity [1]. *Weak antilocalization* (WAL), on the other hand, refers to destructive interference due to rotated spins of the waves in the opposite direction in the presence of spin-orbit coupling (SOC), leading to an enhanced conductivity [2]. WL and WAL have recently been explored in doped ZnO films and nanowires because of potential applications in nano-electronics and spintronics [3–10]. Crossovers from WL to WAL have been observed in magnetoconductivity of InZnO films via temperature variation [7, 9]. However, gate-controlled quantum interference in ZnO or its doped form was not reported until very recently, when competitions between WL and WAL were discovered in single-gate a-IGZO TFTs via electric gating in our previous research [11], and an intriguing universal dependence of the respective WL and WAL contributions on the channel conductivity was observed [12]. In this paper, more information about this universal dependence is revealed by quantum magnetotransport measurements on double-gate a-IGZO TFTs with higher conductivity. This universal dependence is found to be robust against interface disorder, and therefore the conductivity can reliably reveal the strength of the SOC effect tuned by variation of a single or multiple gate voltages of spintronic devices.

The a-IGZO TFTs with an inverted staggered via-contact structure are fabricated on glass as shown in Fig. 1. First, a Mo film was sputtered as bottom gate electrodes, followed by a SiO_x gate insulating layer deposited by plasma-enhanced chemical vapor deposition (PECVD). Next, a 40-nm-thick a-IGZO channel layer was sputtered at room temperature with a targeted $\text{In}_2\text{O}_3:\text{Ga}_2\text{O}_3:\text{ZnO}$ atomic ratio of 1:1:1. A SiO_x etching stop layer was then deposited by PECVD at 200 °C. The via-contact-type source and drain electrodes were formed by sputtering Mo. A $\text{SiO}_x/\text{SiN}_x$ film was deposited as the

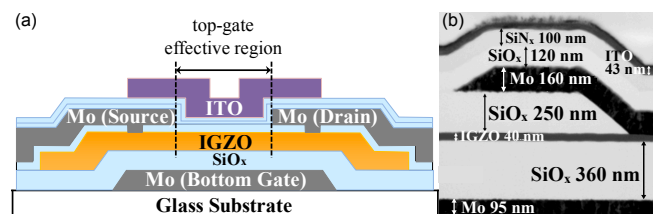


FIG. 1. (a) Schematic drawing and (b) the TEM image of the cross-sectional view of the double-gate a-IGZO thin-film transistor.

passivation layer using PECVD. Indium-tin-oxide (ITO) electrodes were then formed as the top gates. Finally, the device was annealed at 240 °C in an atmospheric oven.

Electrical measurements were performed on several double-gate a-IGZO TFTs. Low-temperature measurements were conducted with the device mounted in a cryogenic system equipped with a superconducting magnet. Connections to the electrodes are made via wire bonding. The data presented in this paper are collected from a representative sample with a channel width (W) of 20 μm and a channel length (L) of 10 μm . Fig. 2a shows I_D under a bottom-gate voltage (V_{BG}) sweep with a grounded top gate, a top-gate voltage (V_{TG}) sweep with a grounded bottom gate, and a double-gate voltage sweep with $V_{BG} = V_{TG}$, respectively. Their respective field-effect mobilities (μ) are displayed in Fig. 2b. The three curves on the left in Fig. 2a are taken at room temperature with $V_D = 0.1$ V. For the V_{BG} sweep with $V_{TG} = 0$, the threshold gate voltage is 1.9 V, the sub-threshold swing is 0.18 V/decade, and $\mu \sim 4.8$ cm^2/Vs and $I_D \sim 0.13$ μA when entering the linear regime. For the double-gate voltage sweep, I_D behaves similarly to that under the V_{BG} sweep, but I_D and μ at the beginning of the linear regime increase to ~ 0.23 μA and ~ 6.4 cm^2/Vs , respectively. If instead V_{TG} is swept with $V_{BG} = 0$, I_D is much smaller than the other two sweeps, and stays almost constant for $V_{TG} > 10$ V. The small constant I_D can be interpreted as the electron-injection-induced diffusion current due to the screening of top-gate electric field by the redundant source and drain electrodes

* E-mail: pjiang@ntnu.edu.tw

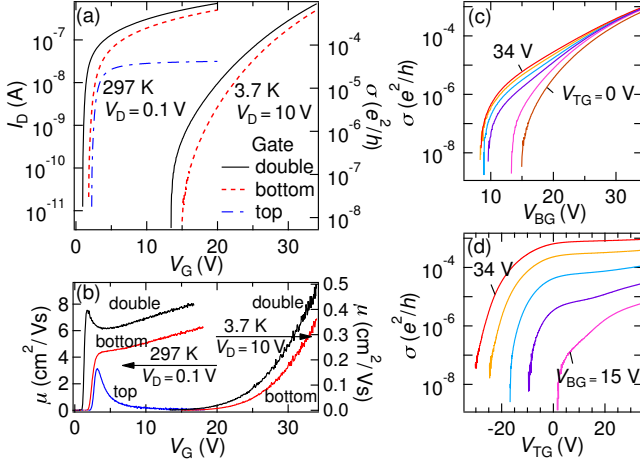


FIG. 2. (a) Drain currents (I_D) as functions of the bottom-, top-, or double-gate voltages. Room-temperature data are taken with a drain voltage (V_D) of 0.1 V, whereas 3.7-K data are taken with $V_D = 10$ V. The corresponding 2D conductivity (σ) is appended on the right axis. (b) Respective field-effect mobilities (μ) as functions of the gate voltages. $\mu = dI_D/dV_G \cdot L/(WC_{\text{ins}}V_D)$, where C_{ins} is the insulating-layer capacitance measured as functions of the bottom-, top-, or double-gate voltages, respectively. μ curves at 3.7 K are appended to the right axis. (c) σ at 3.7 K with $V_D = 10$ V as functions of the bottom-gate voltage (V_{BG}) at various top-gate voltages (V_{TG}) of 0, 10, 20, 25, 30, and 34 V, respectively from bottom to top. (d) σ at 3.7 K with $V_D = 10$ V as functions of V_{TG} at various V_{BG} of 15, 20, 25, 30, and 34 V, respectively from bottom to top.

[13], as illustrated in Fig. 1, leading to an effective length of only $\sim 3/4$ of the channel length [14].

At a low temperature (T) of 3.7 K, the threshold gate voltage is seriously enhanced, and I_D is not detectable with $V_D = 0.1$ V for any gate voltages less than 35 V. Therefore, a larger V_D of 10 V is supplied for all 3.7-K measurements to give detectable I_D [15]. At 3.7 K, I_D increases much more slowly with the gate voltages, as shown in Fig. 2a, and is not even detectable at any V_{TG} below 35 V when $V_{BG} = 0$ because of the extremely low diffusion rate of the carriers. μ is only ~ 0.5 cm^2/Vs when $V_{TG} = V_{BG} = 34$ V, and remains higher under the double-gate voltage sweep than under the V_{BG} sweep. The seriously suppressed μ at low T can be interpreted in the percolation model for amorphous oxide semiconductor TFTs [16, 17]. Shown on the right axis of Fig. 2a is the 2D conductivity (σ) given by $I_D/V_D \cdot L/W$, and is expressed in unit of e^2/h , where h is the Planck's constant.

The conductivity (σ) at 3.7 K was further measured under various combinations of gate voltages. Fig. 2c presents σ vs V_{BG} at various fixed V_{TG} , whereas Fig. 2d shows σ vs V_{TG} at various fixed V_{BG} . It can be seen that the two gates control the carriers in the channel in very different manners. In Fig. 2c, all σ curves of differ-

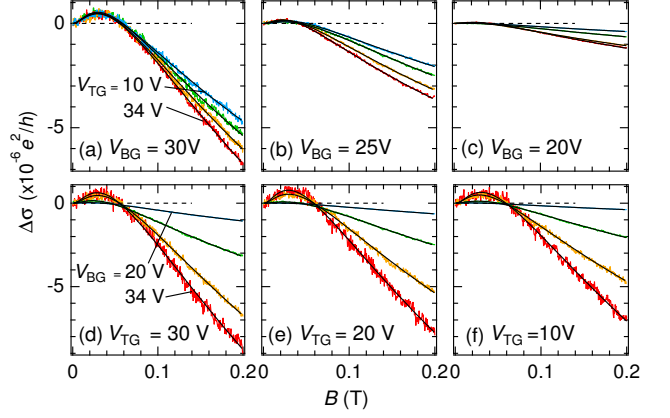


FIG. 3. $\Delta\sigma$ at 3.7 K as functions of the magnetic field (B) (a)–(c) at fixed V_{BG} (30, 25, or 20 V) with various V_{TG} of 10, 20, 30, and 34 V, respectively from top to bottom, and (d)–(f) at fixed V_{TG} (30, 20, or 10 V) with various V_{BG} of 20, 25, 30, and 34 V, respectively from top to bottom. Theoretical fits (Eq. 1) are shown as solid smooth lines.

ent V_{TG} approach an “asymptote” that passes through $\sim 10^{-3}e^2/h$ at $V_{BG} = 34$ V. However, $V_{TG} = 34$ V, as shown in Fig. 2d, gives much smaller values of σ at various smaller V_{BG} until V_{BG} reaches 34 V to give $\sigma \sim 10^{-3}e^2/h$. These results reflect the limited effectiveness of V_{TG} .

The quantum magnetotransport are investigated at 3.7 K with magnetic field (B) perpendicular to the channel plane. The representative curves of $\Delta\sigma(B) (\equiv \sigma(B) - \sigma(0))$ are shown in Fig. 3. Figs. 3a–3c display $\Delta\sigma(B)$ at respective fixed V_{BG} with various V_{TG} from 10 V to 34 V, whereas Figs. 3d–3f display $\Delta\sigma$ at respective fixed V_{TG} with various V_{BG} from 20 V to 34 V. In general, $\Delta\sigma$ curves with higher gate voltages increase with B up to $B \sim 0.037$ T, demonstrating a WL signature, but then bend over to WAL and decrease substantially at higher B . The WL and WAL features are suppressed as either gate voltage is decreased, but with different effectiveness. Fig. 3 shows that varying V_{BG} substantially changes the magnetotransport of the device, whereas varying V_{TG} only tunes it mildly.

To assess the respective contributions of WL and WAL for each $\Delta\sigma(B)$ curve, we use the two-component Hikami–Larkin–Nagaoka (HLN) theory for the magnetoconductivity of a 2D system in the limit of strong SOC [2, 18, 19]:

$$\Delta\sigma(B) = A \sum_{i=0,1} \frac{\alpha_i e^2}{\pi h} \left[\Psi \left(\frac{\ell_B^2}{\ell_{\phi i}^2} + \frac{1}{2} \right) - \ln \left(\frac{\ell_B^2}{\ell_{\phi i}^2} \right) \right], \quad (1)$$

where Ψ is the digamma function, $\ell_B \equiv \sqrt{\hbar/(4e|B|)}$ is half the magnetic length, the prefactors α_0 and α_1 stand for the weights of WL and WAL, respectively, and $\ell_{\phi i}$ is the corresponding phase coherence length. The original two-component HLN equation was proposed for topologi-

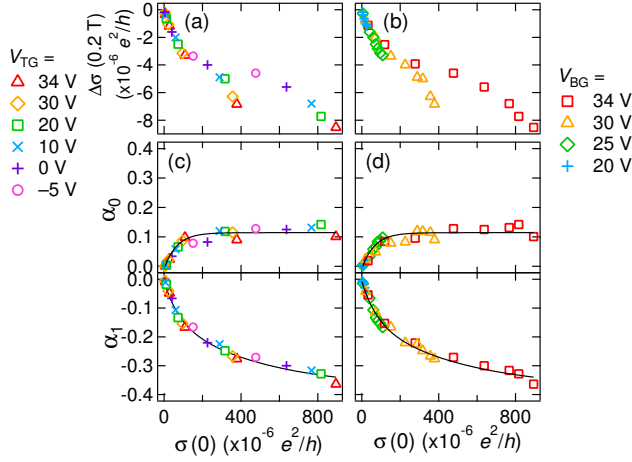


FIG. 4. $\Delta\sigma(0.2 \text{ T})$ vs $\sigma(0)$ (a) at various fixed V_{TG} , and (b) at various fixed V_{BG} . There are duplicate data points in (a) and (b); for example, “+” at $\sigma(0) = 637 \times 10^{-6} e^2/h$ in (a) and “□” at the same $\sigma(0)$ in (b) are the same data point at $V_{TG} = 0$ and $V_{BG} = 34 \text{ V}$. α_0 (the prefactor for WL) and α_1 (the prefactor for WAL) obtained from the theoretical fits (Eq. 1) at various gate voltages used in (a) and (b) are shown in (c) and (d), respectively. Eye-guiding lines of the universal curves are shown as solid smooth lines.

cal insulator thin films [18, 19]. Owing to the percolation conduction in a-IGZO [16], it is believed that the effective L is much larger and the effective W is much smaller than the values of the channel dimensions [20, 21]. This implies that the real conductivity is much larger than $\sigma \equiv I_D/V_D \cdot L/W$. Therefore, we add a small coefficient A to the original equation [18, 19] to address this issue. The magnitudes of σ of the double-gate a-IGZO TFTs are found to be ~ 3 times larger than those of the single-gate a-IGZO TFTs from our previous measurements [11, 12], so A is set to 3×10^{-4} in this work to roughly compensate the difference in sample quality [22]. Eq. 1 provides excellent fits to all the curves in Fig. 3, which are shown as solid smooth lines.

Measurements on the double-gate a-IGZO TFTs with higher $\sigma(0)$ (σ at zero B) allow us to investigate the evolution of the WL and WAL competitions from zero- to high-conductivity regimes. In our previous experiment on single-gate a-IGZO TFTs [12], only low-conductivity transport ($\sigma(0) \lesssim 200 \times 10^{-6} e^2/h$) could be studied. Figs. 4a and 4b display $\Delta\sigma(0.2 \text{ T})$ vs $\sigma(0)$ to demonstrate that different gate operations may give different $\Delta\sigma$ at the same $\sigma(0)$ and B when $\sigma(0)$ is large ($> 200 \times 10^{-6} e^2/h$ for the case of $B = 0.2 \text{ T}$). Fig. 4a shows $\Delta\sigma(0.2 \text{ T})$ at various fixed V_{TG} as functions of $\sigma(0)$ achieved by varying V_{BG} , whereas Fig. 4b shows $\Delta\sigma(0.2 \text{ T})$ at various fixed V_{BG} as functions of $\sigma(0)$ achieved by varying V_{TG} . The values of α_0 and α_1 obtained by fitting experimental $\Delta\sigma(B)$ curves at respective gate voltages to Eq. 1 are plotted against $\sigma(0)$ in Figs. 4c and 4d [23], and each of them surprisingly col-

lapses onto a universal curve despite the distinct patterns of $\Delta\sigma(0.2 \text{ T})$ vs $\sigma(0)$ obtained from different gate operations shown in Figs. 4a and 4b. α_0 increases rapidly from 0 to ~ 0.1 with increasing $\sigma(0)$, but then stays around 0.1 after the transport passes the threshold. $|\alpha_1|$ grows substantially with increasing $\sigma(0)$, and then slows down to approach ~ 0.35 when $\sigma(0)$ gets close to $\sim 10^{-3} e^2/h$. It is noticed that the shape of the universal curve may vary among devices with different structure fabrications. The single-gate a-IGZO TFTs in our previous experiment [12], for example, never entered the linear regime within the V_G range studied, and therefore its partial universal curve of α_1 vs $\sigma(0)$ did not show any changes in the slope.

The values of $\ell_{\phi i}$ obtained by fitting the experimental $\Delta\sigma(B)$ to Eq. 1 fluctuate mildly near $0.1 \mu\text{m}$ as V_{BG} or V_{TG} is varied. A closer look at the dependence of $\ell_{\phi i}$ on $|V_{BG} - V_{TG}|$ reveals that $\ell_{\phi 0}$ decreases from $\sim 0.14 \mu\text{m}$ to $\sim 0.11 \mu\text{m}$ and $\ell_{\phi 1}$ decreases from $\sim 0.10 \mu\text{m}$ to $\sim 0.08 \mu\text{m}$ as $|V_{BG} - V_{TG}|$ is increased from 0 to 54 V. This implies that the transport suffers stronger disorder scattering at larger vertical electric fields. In a temperature-dependence measurement, on the other hand, $\ell_{\phi i}$ is found to decrease by more than a half when T is increased beyond 50 K, which weakens the WL and WAL effects. The dependence of α_i on $\sigma(0)$ also evolves with T [11]. To better observe WL and WAL, $\ell_{\phi i}$ should be much larger than the elastic scattering length (ℓ_e) and than the spin-orbit scattering length (ℓ_{SO}) (i.e., the strong SOC limit). Analyses on our data at 3.7 K using the original HLN equation without the assumption of strong SOC [2, 24, 25] reveal that $(\ell_{\phi i}/\ell_{SO})^2 \sim (\ell_{\phi i}/\ell_e)^2$ ranges from ~ 50 to ~ 160 , which satisfies the conditions for Eq. 1 to be valid, and for the SOC effects to dominate for potential applications in spintronics.

Gate-voltage-controlled competitions between WL and WAL were also discovered in topological insulator thin films [26], and their α_0 and α_1 were theoretically shown to be determined by the ratio of the gap opening at the Dirac point to the Fermi energy [18, 19]. The universal dependence of the competing WL and WAL on $\sigma(0)$ observed in a-IGZO TFT may also find its explanation in the relation between the channel conductivity and the gate-controlled Fermi-level position relative to the band structure, but this is yet to be confirmed by theoretical investigations. The a-IGZO TFTs can be used to tune the SOC effect to a desired weight via electric gating by monitoring $\sigma(0)$ thanks to the universal dependence of α_i on $\sigma(0)$. More research is required for future realization of ZnO-based spin transistors [27] or other spintronic devices.

The double-gate structure offers a better control of the channel potential [28, 29], and thus allows a more comprehensive study. When $V_{BG} = V_{TG}$, the vertical electric field becomes minimal, reducing the interface roughness scattering [30]. This explains why $V_{BG} = V_{TG}$ gives the highest μ as shown in Fig. 2b and the longest $\ell_{\phi i}$ mentioned previously. However, the universal curves of α_i vs $\sigma(0)$ shown in Figs. 4c and 4d are robust at any

$|V_{BG} - V_{TG}|$ regardless of the existence of interface disorder. This implies that, although WL, WAL, and $\sigma(0)$ are all known to be affected by disorder [7, 9], the affected $\sigma(0)$ alone is somehow sufficient to determine the weights of WL and WAL in the system. More theoretical studies are needed to fully understand the underlying physics. The resilience of the universal dependence to interface disorder should be a great advantage for future sophisticated multigate spintronic devices. Once the dependence

of α_i on σ is determined for a TFT structure with a constant a-IGZO channel quality at a constant T , the dependence should hold regardless of different strength of interface roughness scattering caused by different vertical electric fields imposed by gate voltages.

The work was supported by the Ministry of Science and Technology of the Republic of China under Grant No. MOST 102-2112-M-003-009-MY3.

-
- [1] B. L. Altshuler and A. G. Aronov, in “Electron-electron Interactions in Disordered Systems,” edited by A. L. Efros and M. Pollak (Elsevier, Amsterdam, 1985).
- [2] S. Hikami, I. Larkin, and Y. Nagaoka, “Spin-Orbit Interaction and Magnetoresistance in the Two Dimensional Random System,” *Prog. Theor. Phys.*, vol. 63, no. 2, pp. 707–710, Feb. 1980. DOI: 10.1143/PTP.63.707.
- [3] Ü. Özgür, Y. I. Alivov, C. Liu, A. Teke, M. A. Reshchikov, S. Doğan, V. Avrutin, S.-J. Cho, and H. Morkoç, “A comprehensive review of ZnO materials and devices,” *J. Appl. Phys.*, vol. 98, no. 98, pp. 041301–1–041301-103, Aug. 2005. DOI: 10.1063/1.1992666.
- [4] B. Shinozaki, K. Makise, Y. Shiname, H. Nakamura, and K. Inoue, “Weak localization and electron–electron interaction effects in indium zinc oxide films,” *J. Phys. Soc. Jpn.*, vol. 76, no. 7, pp. 074718–1–074718-6, Jul. 2007. DOI: 10.1143/JPSJ.76.074718.
- [5] R. Thompson, D. Li, C. Witte, and J. Lu, “Weak localization and electron-electron interactions in indium-doped ZnO nanowires,” *Nano Lett.*, vol. 9, no. 12, pp. 3991–3995, Oct. 2009. DOI: 10.1021/nl902152c.
- [6] X. Xu, A. C. Irvine, Y. Yang, X. Zhang, and D. A. Williams, “Coulomb oscillations of indium-doped ZnO nanowire transistors in a magnetic field,” *Phys. Rev. B*, vol. 82, no. 19, pp. 195309–1–195309-5, Nov. 2010. DOI: 10.1103/PhysRevB.82.195309.
- [7] B. Shinozaki, K. Hidaka, S. Ezaki, K. Makise, T. Asano, S. Tomai, K. Yano, and H. Nakamura, “Crossover from weak localization to anti-weak localization in indium oxide systems with wide range of resistivity,” *J. Appl. Phys.*, vol. 113, no. 15, pp. 153707–1–153707-6, Apr. 2013. DOI: 10.1063/1.4801809.
- [8] S.-P. Chiu, J. G. Lu, and J.-J. Lin, “Quantum-interference transport through surface layers of indium-doped ZnO nanowires,” *Nanotechnology*, vol. 24, no. 24, pp. 245203–1–245203-14, May 2013. DOI:10.1088/0957-4484/24/24/245203.
- [9] H. Yabuta, N. Kaji, M. Shimada, T. Aiba, K. Takada, H. Omura, T. Mukaide, I. Hirose, T. Koganezawa, and H. Kumomi, “Microscopic structure and electrical transport property of sputter-deposited amorphous indium-gallium-zinc oxide semiconductor films,” *J. Phys.: Conf. Ser.*, vol. 518, no. 1, pp. 012001–1–012001-12, Jun. 2014. DOI:10.1088/1742-6596/518/1/012001.
- [10] V. A. Kulbachinskii, V. G. Kytin, O. V. Reukova, L. I. Burova, A. R. Kaul, and A. G. Ulyashin, “Electron transport and low-temperature electrical and galvanomagnetic properties of zinc oxide and indium oxide films,” *Low Temp. Phys.*, vol. 41, no. 2, pp. 116–124, Feb. 2015. DOI: 10.1063/1.4908194.
- [11] W.-H. Wang, S.-R. Lyu, E. Heredia, S.-H. Liu, P. Jiang, P.-Y. Liao, T.-C. Chang, and H.-M. Chen, “Competing weak localization and weak antilocalization in amorphous indium–gallium–zinc-oxide thin-film transistors,” *Appl. Phys. Lett.*, vol. 110, no. 2, pp. 022106–1–022106-4, Jan. 2017. DOI: 10.1063/1.4974080.
- [12] W.-H. Wang, S.-R. Lyu, E. Heredia, S.-H. Liu, P. Jiang, P.-Y. Liao, and T.-C. Chang, “Universal dependence on the channel conductivity of the competing weak localization and antilocalization in amorphous InGaZnO4 thin-film transistors,” *Appl. Phys. Express*, vol. 10, no. 5, pp. 051103–1–051103-4, Apr. 2017. DOI: 10.7567/APEX.10.051103.
- [13] M.-Y. Tsai, T.-C. Chang, A.-K. Chu, T.-Y. Hsieh, C.-E. Chen, H.-M. Chen, P.-Y. Liao, B.-W. Chen, Y.-X. Yang, K.-K. Chen, T.-H. Shih, and H.-H. Lu, “Investigating the degradation behaviors for bottom/top gate sweep under negative bias illumination stress in dual gate InGaZnO thin film transistors,” *SID Digest*, vol. 46, no. 1, pp. 1147–1150, Jun. 2015. DOI: 10.1002/sdtp.10033.
- [14] P.-Y. Liao, T.-C. Chang, T.-Y. Hsieh, M.-Y. Tsai, B.-W. Chen, A.-K. Chu, C.-H. Chou, and J.-F. Chang, “Investigating degradation behavior of hole-trapping effect under static and dynamic gate-bias stress in a dual gate a-InGaZnO thin film transistor with etch stop layer,” *Thin Solid Films*, vol. 603, no. 31, pp. 359–362, Mar. 2016. DOI: 10.1016/j.tsf.2016.01.035.
- [15] A V_D larger than $(V_G - V_{\text{threshold}})$ is expected to pinch off the channel near the drain. However, I_D of the a-IGZO TFTs at low T stays in the linear regime even when $V_D = 10$ V, which is much higher than $(V_G - V_{\text{threshold}})$ [11]. Therefore, σ is assumed to be independent of the position in the channel.
- [16] H. Hosono, “Ionic amorphous oxide semiconductors: Material design, carrier transport, and device application,” *J. Non-Cryst. Solids*, vol. 352, no. 9, pp. 851–858, Apr. 2006. DOI: 10.1016/j.jnoncrysol.2006.01.073.
- [17] S. Lee, A. Nathan, J. Robertson, K. Ghaffarzadeh, M. Pepper, S. Jeon, C. Kim, I.-H. Song, U.-I. Chung, and K. Kim, “Temperature dependent electron transport in amorphous oxide semiconductor thin film transistors,” *IEEE IEDM Dig. Tech. Papers*, pp. 14.6.1–14.6.4, DOI: 10.1109/IEDM.2011.6131554.
- [18] H. Z. Lu, J. Shi, and S. Q. Shen, “Competition between Weak Localization and Antilocalization in Topological Surface States,” *Phys. Rev. Lett.*, vol. 107, no. 7, pp. 076801–1–076801-5, Aug. 2011. DOI: 10.1103/PhysRevLett.107.076801.

- [19] H. Z. Lu, and S. Q. Shen, “Weak localization of bulk channels in topological insulator thin films,” *Phys. Rev. B.*, vol. 84, no. 12, pp. 125138-1–125138-8, Sep. 2011. DOI: 10.1103/PhysRevB.84.125138.
- [20] B. Shinozaki, S. Ezaki, K. Hidaka, K. Makise, T. Asano, K. Yano, and H. Nakamura, “Weak localization and percolation effects in annealed In_2O_3 – ZnO thin films,” *AIP Adv.*, vol. 1, no. 3, pp. 032149-1–032149-6, Aug. 2011. DOI: 10.1063/1.3635375.
- [21] T. Kamiya, K. Nomura, and H. Hosono, “Electronic structures above mobility edges in crystalline and amorphous In-Ga-Zn-O : Percolation conduction examined by analytical model,” *J. Display Technol.*, vol. 5, no. 12, pp. 462–467, Dec. 2009. DOI: 10.1109/JDT.2009.2022064.
- [22] The value of A represents the homogeneity of each sample [20]. The estimated value of A could be a constant factor off, but it would not change the fact that α_i vs $\sigma(0)$ falls onto a universal curve to be presented later.
- [23] Uncertainty in fitting to Eq. 1 increases near $\sigma(0) = 0$ because $\Delta\sigma(B)$ approaches zero, showing a flat, *unitary*-like behavior [2] with $\alpha_0 \approx -\alpha_1$. The values of α_i near $\sigma(0) = 0$ are carefully extracted from fitting by minimizing the standard deviations and modeling the evolution of the dominating WAL feature based on the fitting results at higher $\sigma(0)$.
- [24] S. Maekawa, and H. Fukuyama, “Magnetoresistance in two dimensional disordered systems: effects of Zeeman splitting and spin-orbit scattering,” *J. Phys. Soc. Jpn.*, vol. 50, No. 8, pp. 2516–2524, Aug. 1981. DOI: 10.1143/JPSJ.50.2516.
- [25] L. Fang, J. Im, W. DeGottardi, Y. Jia, A. Glatz, K.A. Matveev, W.-K. Kwok, G.W. Crabtree, and M.G. Kanatzidis, “Large spin-orbit coupling and helical spin textures in 2D heterostructure $[\text{Pb}_2\text{BiS}_3][\text{AuTe}_2]$,” *Sci. Rep.*, vol. 6, pp. 35313-1–35313-7, Oct. 2016. DOI: 10.1038/srep35313.
- [26] M. Lang, L. He, X. Kou, P. Upadhyaya, Y. Fan, H. Chu, Y. Jiang, J. Bardarson, W. Jiang, E. S. Choi, Y. Wang, N.-C. Yeh, J. Moore, and K. Wang, “Competing weak localization and weak antilocalization in ultrathin topological insulators,” *Nano Lett.*, vol. 13, no. 1, pp. 48–53, Nov. 2013. DOI: 10.1021/nl303424n.
- [27] S. Datta and B. Das, “Electronic analog of the electro-optic modulator,” *Appl. Phys. Lett.*, vol. 56, no. 7, pp. 665–667, Feb. 1990. DOI: 10.1063/1.102730.
- [28] N. Münzenrieder, C. Zysset, L. Petti, T. Kinkeldei, G. A. Salvatore, and G. Tröster, “Flexible double gate a-IGZO TFT fabricated on free standing polyimide foil,” *Solid-State Electron.*, vol. 84, pp. 198204, Jun. 2013. DOI: 10.1016/j.sse.2013.02.025.
- [29] S. Zhang, R. Han, J.K.O. Sin, and M. Chan, “A novel self-aligned double-gate TFT technology,” *IEEE Electron Device Letters*, vol. 22, no. 11, pp. 530–532, Nov. 2001. DOI: 10.1109/55.962653.
- [30] H. S. P. Wong, D. J. Frank, P. M. Solomon, C. H. J. Wann, and J. J. Welser, “Nanoscale CMOS,” *Proc. IEEE*, vol. 87, no. 4, p. 550, 1999. DOI: 10.1109/5.752515.